Pr^{3+}- and Pr^{3+}/Er^{3+}-Doped Selenide Glasses for Potential 1.6 μm Optical Amplifier Materials

Yong Gyu Choi, Bong Je Park, Kyong Hon Kim, and Jong Heo

1.6 μm emission originated from Pr^{3+}: ($^3F_3$, $^3F_4$) → $^3H_4$ transition in Pr^{3+}- and Pr^{3+}/Er^{3+}-doped selenide glasses was investigated under an optical pump of a conventional 1480 nm laser diode. The measured peak wavelength and full-width at half-maximum of the fluorescent emission are ~1650 nm and ~120 nm, respectively. A moderate lifetime of the thermally coupled upper manifolds of ~212 ± 10 μs together with a high stimulated emission cross-section of ~(3 ± 1)×10^{-20} cm^2 promises to be useful for 1.6 μm band fiber-optic amplifiers that can be pumped with an existing high-power 1480 nm laser diode. Codoping Er^{3+} enhances the emission intensity by way of a nonradiative Er^{3+}: $^4I_{13/2}$ → Pr^{3+}: ($^3F_3$, $^3F_4$) energy transfer. The Dexter model based on the spectral overlap between donor emission and acceptor absorption describes well the energy transfer from Er^{3+} to Pr^{3+} in these glasses. Also discussed in this paper are major transmission loss mechanisms of a selenide glass optical fiber.

Manuscript received September 15, 2000; revised August 1, 2001.

Yong Gyu Choi (phone: +82 42 860 5774, e-mail: ygchoi@etri.re.kr), Bong Je Park (e-mail: bjpark@etri.re.kr), and Kyong Hon Kim (e-mail: kyongh@etri.re.kr) are with the Telecommunication Basic Research Laboratory, Electronics and Telecommunications Research Institute, Daejeon, Korea.

Jong Heo (e-mail: jheo@postech.ac.kr) is with the Department of Materials Science and Engineering, Pohang University of Science and Technology, Pohang, Kyungbuk, Korea.

I. INTRODUCTION

Optical communication bandwidths are limited by the clarity of the transmission window in the SiO_2-based optical fiber. By virtue of recent development of elaborated processing technologies, mass production of OH^--free silica optical fibers which have transparent characteristics in the entire spectrum from ~1200 to ~1700 nm is currently available [1]. Thus, in order to fully utilize the whole transparent region of the dry fibers for large capacity optical communication systems of several tens Tb/s, optical amplifiers covering the wavelengths from shorter than 1300 nm to about 1700 nm are necessary.

Recently, a significant technical improvement has been made in Raman fiber amplifiers and semiconductor optical amplifiers as well as rare-earth (RE) doped fiber amplifiers. However, the RE doped fiber amplifiers have several superior characteristics over the Raman and semiconductor amplifiers. Some of them are possibilities to have a relatively high signal-to-noise ratio, good gain stability, and low signal crosstalk [2]. This paper deals only with fiber materials related to new RE doped fiber amplifiers. Erbium ions doped in either germano-silicate or tellurite glasses have been well demonstrated to provide signal amplification over the wavelength region of 1530 to 1600 nm [3]-[5]. Praseodymium and dysprosium ions are proven to be useful for amplifiers in the 1.3 μm band [6], [7]. Thulium ions in fluoride glasses amplify optical signals in the wavelengths of 1450 to 1520 nm [8] and of longer than 1650 nm [9]. So far, there has been no RE-host combination optimized for optical amplifiers in wavelength regions around 1350 to 1450 nm where the hydroxyl ions cause an additional absorption in the conventional silica fibers, and around 1610 to 1650 nm where the gain-shifted erbium-doped fiber amplifiers cannot provide a practical optical gain. In this paper, we report measured results of spec-

troscopic properties of a Pr^{3+}-doped low phonon energy glass, which is considered as a possible candidate material for 1.6 μm band fiber amplifiers. Sensitizing effect of Er^{3+} on the 1.6 μm emission from the Pr^{3+}-doped glass for optical pump at around 1480 nm is also discussed.

Magnitude of multiphonon relaxation is one of the parameters that govern emission intensity of some radiative intra-4f-configurational transitions of RE ions in a dielectric medium. One representative example of such transitions is the 1.3 μm emission originated from the Pr^{3+}: $^1G_4 \rightarrow {}^3H_5$ transition [6]. The Pr^{3+} ion actually has a luminescence centered at about 1.6 μm from ($^3F_3$, $^3F_4$) $\rightarrow {}^3H_4$ transition, but due to the tightly spaced energy levels of an energy gap of ~1350 cm^{-1}, the radiative transition is virtually forbidden in most glasses, even in sulfide glasses [10]. A lasing action at ~1.6 μm has been demonstrated by using this transition in $LaCl_3$ crystal [11], but no detailed spectroscopic data on this transition from a glass host have been reported yet [12].

The multiphonon relaxation process from the ($^3F_3$, $^3F_4$) level can be reduced in glasses having lower vibrational phonon energy than the sulfide glasses (~350 cm^{-1}) [13], [14]. Some germano-selenide glass systems have thermal stability good enough to be drawn into a fiber waveguide without any crystallization [15], and possess the most intense phonon energy at about 200 cm^{-1} [16]. In this study, we used Ge-As-Ga-Se glasses, and regarded them as a representative of selenide glasses.

II. EXPERIMENTAL

Ge_{30}-As_8-Ga_2-Se_{60} (mol%) composition was used as a host glass. Glasses were prepared from Ge, Ga, As, and Se powders with a purity better than 99.999%. Metals of praseodymium and erbium with purity of 99.999% were used as a starting material of rare-earths. Up to 1 mol% praseodymium could be solved in the host. Introduction of small amount of gallium to the Ge-As-Se system enhanced the RE solubility as did it in Ge-As-S glasses [17]. Approximately 15-g batches were weighed in an Ar-purged glove box with O_2 and OH^- concentrations less than 2 ppm and 5 ppm, respectively. Silica ampoules containing the starting materials were sealed, and melted in a rocking furnace. Temperature was first increased to 500 ℃ with a heating rate of 2 ℃/min and then subsequently elevated to 1000 ℃ by 1 ℃/min. After the melting at 1000 ℃ for 12 h, ampoules with the melt inside were removed from the furnace and quenched into water. Samples were annealed at around their glass transition temperatures (~360 ℃) for two hours. Approximately 2 mm-thick discs were sliced and optically polished for the measurements.

A UV/VIS/NIR spectrophotometer and an FTIR spectrometer were used to measure absorption and transmission spectra in the regions of 500 to 2500 nm and 400 to 4000 cm^{-1}, respectively. A conventional 1480 nm laser diode was used as an excitation source. The emission signals were detected using an arrangement equipped with a 0.5-m monochromator, InGaAs PIN detector, lock-in amplifier and a computer. Re-absorption of the fluorescences was minimized by focusing the excitation beam immediately below the surface of the samples and letting the emitted lights travel the shortest distance inside the sample. Decay traces were monitored with a 500 MHz digitizing oscilloscope at a proper mechanical chopper frequency. A decay lifetime (or duration time) was determined as the first e^{-1}-folding time of the fluorescence emission intensity.

III. RESULTS

1. Absorption Properties

UV-side absorption spectrum of a 1 mol% Pr^{3+}-doped selenide glass is shown in Fig. 1. Host absorption starts at around 800 nm. Shown in Fig. 2 is IR-side transmission spectrum of a Pr^{3+}-doped selenide glass. Transmission cutoff of the host glass appears at ~600 cm^{-1}, which suggests that this glass consists of lower phonon vibration modes than the conventional sulfide glasses. Based on the measured absorption and transmission spectra, one can draw a schematic energy level diagram of Pr^{3+} in these glasses as shown in Fig. 3. The $^3F_4$ and $^3F_2$ multiplets are thermally coupled with the $^3F_3$ and $^3H_6$ levels, respectively [18]. The Boltzmann distribution predicts that approximately

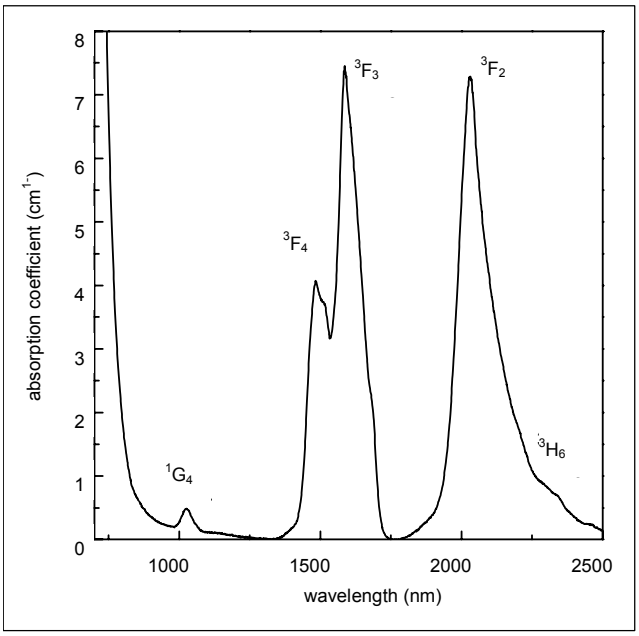

Fig. 1. Absorption spectrum of a 1.0 mol% Pr^{3+}-doped selenide glass.

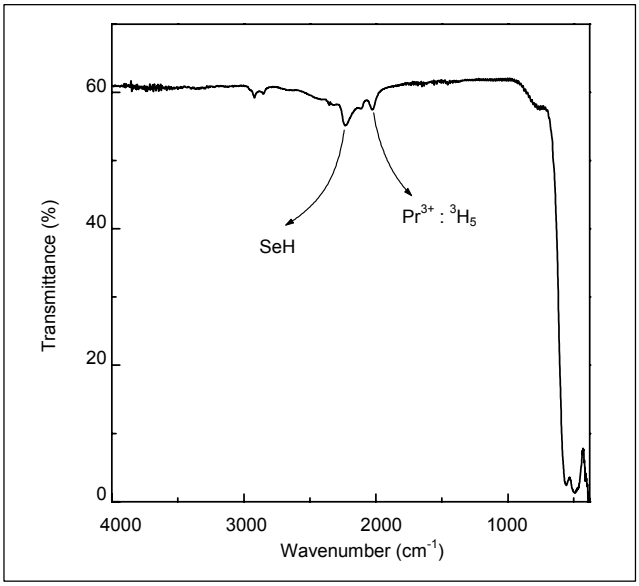

Fig. 2. Infrared transmission spectrum of a Pr^{3+}-doped selenide glass.

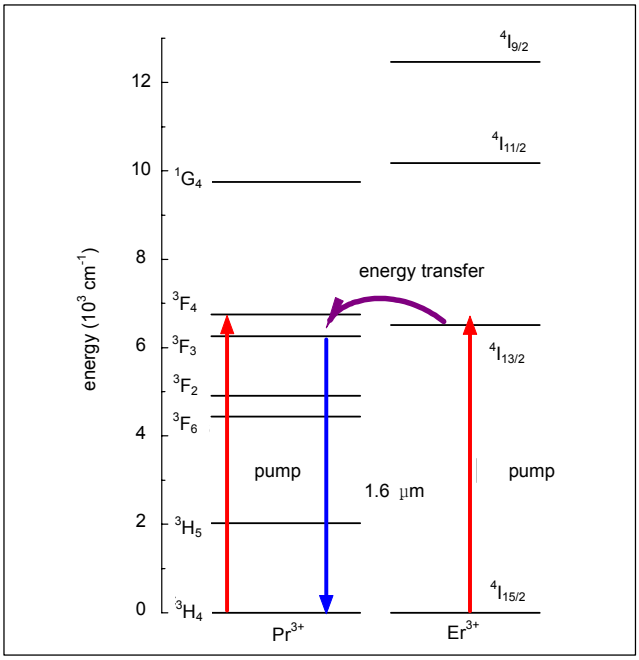

Fig. 3. Schematic energy level diagram of Pr^{3+} and Er^{3+} in selenide glass.

90% and 91% of populations reside in the corresponding lower-lying levels, *i.e.*, $^3F_3$ and $^3H_6$, in this selenide glass, respectively. Thus, we consider the first two thermally coupled manifolds as a ($^3F_3$, $^3F_4$) level, and the other two manifolds as a ($^3F_2$, $^3H_6$) level. Absorption cross-section spectra of the Pr^{3+}: $^3H_4 \rightarrow (^3F_3, ^3F_4)$ and Er^{3+}: $^4I_{15/2} \rightarrow {}^4I_{13/2}$ transitions are presented in Fig. 4. The absorption cross-section of Pr^{3+} peaks at ~1585 nm with a value of ~2.2×10^{-20} cm^2, and at 1480 nm it is ~1.2×10^{-20} cm^2.

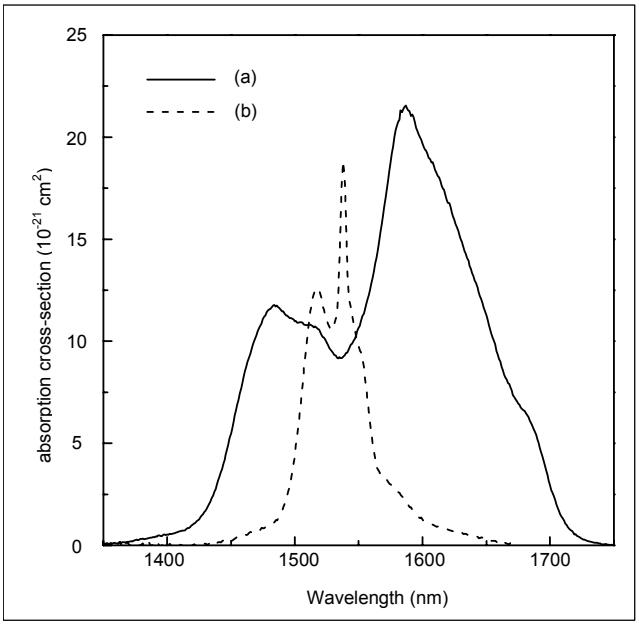

Fig. 4. Absorption cross-section spectra of (a) Pr^{3+}: $^3H_4 \rightarrow (^3F_3, ^3F_4)$ and (b) Er^{3+}: $^4I_{15/2} \rightarrow {}^4I_{13/2}$ in selenide glass.

Meanwhile, the maximum absorption cross-section of Er^{3+} is ~1.9×10^{-20} cm^2 at 1538 nm.

Judd-Ofelt analysis was done using five absorption transitions. Lineshape spectra of the ($^3F_4$, $^3F_3$) and ($^3F_2$, $^3H_6$) manifolds were divided into four corresponding individual transitions with the assumption that each transition appeared to have a Lorentzian lineshape [12]. Three Judd-Ofelt intensity parameters, *i.e.*, Ω_2, Ω_4 and Ω_6 [19] were calculated to be 1.01, 10.54 and 2.53 in 10^{-20} cm^2, respectively. Uncertainty involved in the analysis was estimated to be ~15%. Arranged in Table 1 are the radiative transition probabilities, branching ratio, and radiative lifetimes of some interested transitions. Branching ratio of the 1.6 μm emission is at ~77%.

2. Emission from Single Doped Glasses

Figure 5(a) shows the emission spectrum originated from the ($^3F_3$, $^3F_4$) $\rightarrow$ $^3H_4$ transition. The peak wavelength and full-width at half-maximum are ~1650 nm and ~120 nm, respectively. The peak emission cross-section is about $(3\pm1)\times10^{-20}$ cm^2, which is mostly attributed to high refractive index of the host (~2.5) at near-infrared wavelengths. The Lorentzian local field correction factor represented in terms of refractive index should be incorporated when an electric dipole induced light emission of a rare-earth ion embedded in a dielectric medium is considered. Thus, based on Judd-Ofelt formalism, emission cross-section of a certain manifold is proportional to refractive index of the dielectric medium. Measured lifetimes of the fluorescing level are shown in Fig. 6. Up to 0.05 mol% (~1.7×10^{19} ions/cm^3) of Pr^{3+} the

Table 1. Results of Judd-Ofelt analysis performed on a Pr^{3+}-doped Ge_{30}-As_8-Ga_2-Se_{60} glass.

transition	wavelength (μm)	radiative transition probability* (s^{-1})	branching ratio (%)	calculated lifetime (ms)
$^3H_5 \rightarrow {}^3H_4$	4.9	43	100	23.0
$^3H_6 \rightarrow {}^3H_5$	4.5	52	48	9.1
$^3H_6 \rightarrow {}^3H_4$	2.4	57	52	
$^3F_2 \rightarrow {}^3H_6$	1.4	1	~0	0.447
$^3F_2 \rightarrow {}^3H_5$	3.4	360	16	
$^3F_2 \rightarrow {}^3H_4$	2.0	1873	84	
$^3F_3 \rightarrow {}^3F_2$	7.2	3	~0	0.272
$^3F_3 \rightarrow {}^3H_6$	4.8	104	3	
$^3F_3 \rightarrow {}^3H_5$	2.3	743	20	
$^3F_3 \rightarrow {}^3H_4$	1.6	2836	77	
$^3F_4 \rightarrow {}^3F_3$	2.2	~0	~0	0.500
$^3F_4 \rightarrow {}^3F_2$	5.4	3	~0	
$^3F_4 \rightarrow {}^3H_6$	3.9	251	13	
$^3F_4 \rightarrow {}^3H_5$	2.1	871	43	
$^3F_4 \rightarrow {}^3H_4$	1.5	880	44	
$^1G_4 \rightarrow {}^3F_4$	3.4	85	4	0.450
$^1G_4 \rightarrow {}^3F_3$	3.0	9	~0	
$^1G_4 \rightarrow {}^3F_2$	2.0	31	1	
$^1G_4 \rightarrow {}^3H_6$	1.8	751	34	
$^1G_4 \rightarrow {}^3H_5$	1.3	1216	55	
$^1G_4 \rightarrow {}^3H_4$	1.0	127	6	

* Magnetic dipole transition is not considered, and error involved in the calculations is ~15%.

upper level lifetime is nearly constant to be ~212 ± 10 μs, whereas the lifetime decreases as the concentration further increases. The concentration quenching mechanisms acting on the ($^3F_3$, $^3F_4$) manifolds are probably cross-relaxation processes corresponding to either ($^3F_3$, $^3F_4$) : $^3H_5 \rightarrow$ ($^3F_2$, $^3H_6$) : ($^3F_2$, $^3H_6$) or ($^3F_3$, $^3F_4$) : $^3H_4 \rightarrow$ ($^3F_2$, $^3H_6$) : $^3H_5$ [20]. Therefore, the Pr^{3+} concentration should be kept lower than 0.05 mol% to minimize the concentration quenching.

3. Emission from Codoped Glasses

We added Er^{3+} into the Pr^{3+}-doped glasses as a sensitizer to enhance the excitation efficiency of the 1480 nm pumping. Figure 5(b) shows a typical emission spectrum of Pr^{3+}/Er^{3+}-codoped glasses. The emission intensity increases with the introduction of Er^{3+}. To confirm energy transfer from Er^{3+} to Pr^{3+}, duration times of the codoped samples were measured at 1650 nm for the ($^3F_3$, $^3F_4$) level and at 1535 nm for the Er^{3+}: $^4I_{13/2}$ level. Figure 7 shows the measured duration times of the two manifolds under pumping at 1480 nm. Lifetime of the Er^{3+}: $^4I_{13/2}$ level decreases as the Er^{3+} concentration increases in the codoped samples, while the apparent duration time of the Pr^{3+}: ($^3F_3$, $^3F_4$) level increases. Lifetimes of the $^4I_{13/2}$ level in Er^{3+}-single-doped and Pr^{3+}/Er^{3+}-codoped glasses where Er^{3+} concentration is 0.1 mol% are ~3.26 ms and ~0.75 ms, respectively. This confirms that a fast energy transfer between the Er^{3+}: $^4I_{13/2}$ and Pr^{3+}: ($^3F_3$, $^3F_4$) levels takes place as illustrated in Fig. 3. On the other hand, the lifetime increase of the ($^3F_3$, $^3F_4$) level is dedicated to the prolonged population feeding from the Er^{3+}: $^4I_{13/2}$ even after stop of the excitation. The maximum Er^{3+} concentration can be determined in consideration of magnitude of the $^4I_{15/2} \rightarrow {}^4I_{13/2}$ ground state absorption at the 1.6 μm band and RE solubility of the host.

A direct excitation to the upper Stark levels of the ($^3F_3$, $^3F_4$)

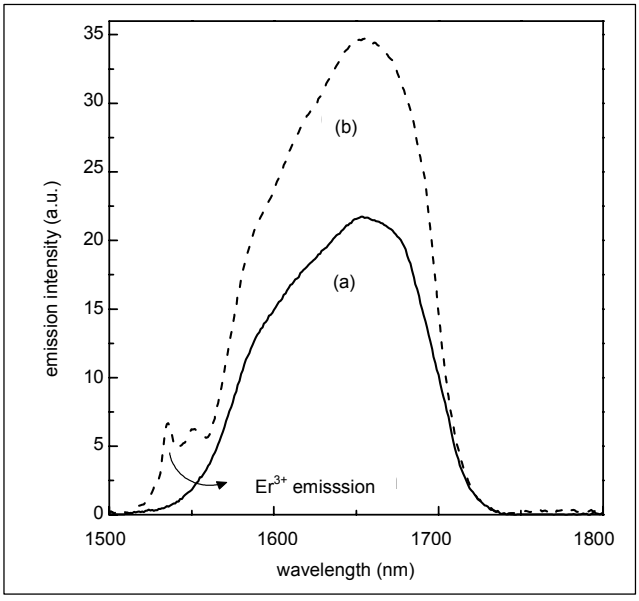

Fig. 5. Emission spectra of 0.05 mol% Pr^{3+}-doped glasses, where codoped Er^{3+} concentration is (a) 0 and (b) 0.2 mol%.

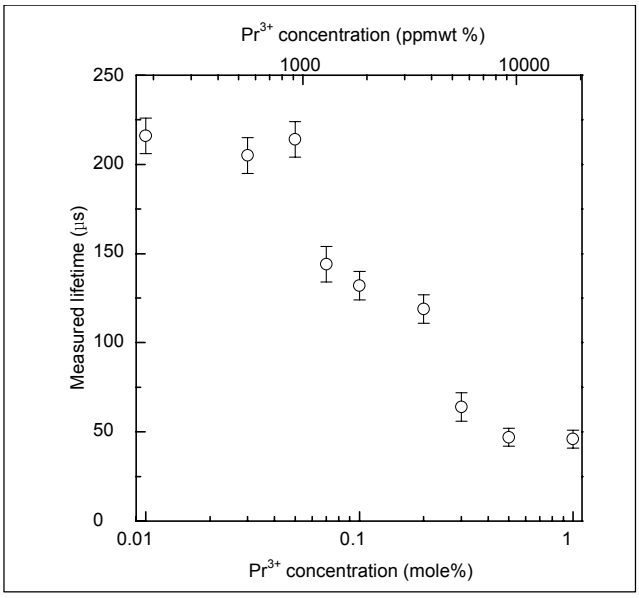

Fig. 6. Measured lifetimes of the ($^3F_3$, $^3F_4$) manifolds against Pr^{3+} concentrations.

multiplet is preferred to make an efficient emission at 1.6 μm because the UV-side absorption of the host starts at around 800nm as shown in Fig. 1. If excited with a 1.5 μm pump source instead of the 1480 nm one, Pr^{3+}/Er^{3+}-codoped glasses may emit the 1.6 μm luminescence with a greater intensity.

IV. DISCUSSION

1. Energy Transfer from Er^{3+} to Pr^{3+}

According to the Dexter's classical theory on the nonradiative energy transfer, overlap of spectral lineshapes between the energy-donor emission and acceptor absorption plays a crucial role in determining the magnitude of electric multipole-induced nonradiative energy transfers [21]. A quantitative analysis involving other parameters such as integrated absorption cross-section of the energy-accepting level and energy migration among donors can be done [19], but it is not considered in this paper. Normalized lineshape spectra of the emission and absorption transitions of Er^{3+}: $^4I_{13/2} \leftrightarrow {}^4I_{15/2}$ and Pr^{3+}: $^3H_4 \leftrightarrow (^3F_3, {}^3F_4)$ are shown in Fig. 8. The overlapped area is much larger in the forward $Er^{3+} \rightarrow Pr^{3+}$ transfer than in the backward case. Thus, it is evident that the forward energy transfer, i.e., Er^{3+}: $^4I_{13/2} \rightarrow Pr^{3+}$: ($^3F_3$, $^3F_4$), would be much faster than the backward Pr^{3+}: ($^3F_3$, $^3F_4$) $\rightarrow Er^{3+}$: $^4I_{13/2}$ transfer. The agile energy transfer of Er^{3+}: $^4I_{13/2}$ $\rightarrow Pr^{3+}$: ($^3F_3$, $^3F_4$) evidenced by this static spectroscopic consideration is further confirmed by the data related to the variations of measured lifetimes of the Er^{3+}: $^4I_{13/2}$ and Pr^{3+}: ($^3F_3$, $^3F_4$) levels. Lifetime of the Er^{3+}: $^4I_{13/2}$ level abruptly decreases as shown in Fig. 9 when Pr^{3+} ions are introduced. The decay trace of the $^4I_{13/2}$ level in a 0.1 mol% Er^{3+}-single-doped glass shows a nearly exponential behavior with a e^{-1} folding lifetime of ~3.26 ms, while a nonexponential decay curve appears when 0.05 mol% of Pr^{3+} codopes the Er^{3+}-single-doped glass, and at the same time the lifetime becomes ~0.75 ms. The nonexponentiality in a decay trace usually results from a nonradiative energy transfer [22].

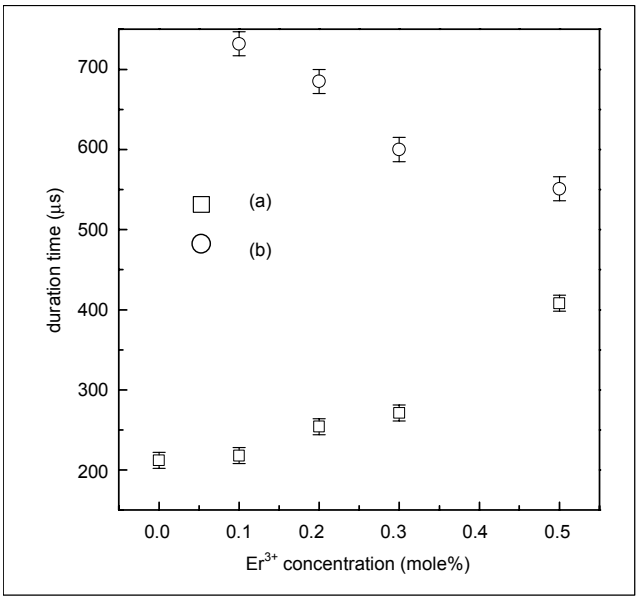

Fig. 7. Duration times of (a) Pr^{3+}: ($^3F_3$, $^3F_4$) and (b) Er^{3+}: $^4I_{13/2}$ levels in Pr^{3+}/Er^{3+}-codoped glasses. Pr^{3+} concentration is fixed at 0.05 mol%. Note that the first e^{-1}-folding times in codoped samples are influenced by population feeding from Er^{3+} to Pr^{3+} occurring even after stop of excitation. Thus, the first e^{-1}-folding times indicate duration times in the case of codoped samples.

Table 2. Representative phonon energy ($\hbar\varpi$), calculated lifetime (τ_0), measured lifetime (τ_m), branching ration (β), quantum efficiency (η), and product of measured lifetime and emission cross-section ($\sigma_{se}\tau_m$) associated with the 1.3 μm and 1.6 μm emissions in some Pr^{3+}-doped low phonon energy glasses.

glasses	transition	$\hbar\varpi$ (cm-1)	τ_0 (μs)	τ_m (μs)	β (%)	η (%)	$\sigma_{se}\tau_m$ (10^{-26} cm^2s)
fluoride*	$^1G_4 \rightarrow {}^3H_5$	~500	2484	110	60	4	36
sulfide**	$^1G_4 \rightarrow {}^3H_5$	~350	510	300	52	60	250
selenide***	$(^3F_3, {}^3F_4) \rightarrow {}^3H_4$	~200	~320 ± 50	212 ± 10	~77	65 ± 20	636 ± 200

*ZBLAN [24], **Ga-La-S [25], ***Ge-As-Ga-Se, this work

Also, a rough estimation on the energy transfer rate (W_{et}) can be calculated using the following [23]:

$$W_{et} = 1 - \frac{\tau_c}{\tau_s},$$

where τ_s and τ_c denote the lifetimes without and with an energy acceptor, respectively. Therefore, the energy transfer rate of Er^{3+}: $^4I_{13/2} \rightarrow Pr^{3+}$: $(^3F_3, {}^3F_4)$ becomes ~77%.

2. Characteristics of the 1.6 μm Emission

As a suitable host of Pr^{3+} ion for the 1.3 μm amplifiers, glasses with a low phonon energy are requested to enhance the fluorescing level lifetime. So far, fluoride and sulfide glasses have been considered as a host of the 1.3 μm amplifiers. As stated in Introduction section, the 1.6 μm emission is virtually forbidden even in a sulfide glass, so that some characteristic parameters associated with the Pr^{3+}: $^1G_4 \rightarrow {}^3H_5$ transition in fluoride and sulfide glasses are compared with those of the $(^3F_3, {}^3F_4) \rightarrow {}^3H_4$ transition in the current selenide glass in Table 2. Intrinsic radiative lifetime of the $(^3F_3, {}^3F_4)$ level was estimated in consideration of the population distribution. Product of measured lifetime (τ_m) and emission cross-section (σ_{se}) is a useful figure of merit from which one can evaluate the efficiency of an optical fiber amplifier [26]. As shown in Table 2, the value of $\sigma_{se}\tau_m$ for the selenide glass is higher than that for the sulfide glass. It is because, in the selenide glasses, the emission cross-section is much higher than that of the sulfide glasses, even though both of the glasses feature similar fluorescing level lifetimes.

Oscillator strength of the Pr^{3+}: $^3H_4 \rightarrow {}^1G_4$ transition is much weaker than that of the $^3H_4 \rightarrow (^3F_3, {}^3F_4)$. Moreover, the 1.3 μm-fluorescing $^1G_4$ manifold is located at about ~1020 nm, where no commercial high-power laser diodes are currently available. However, strong and stable laser diodes operating at 1480 nm have been well developed and can be effectively used as pump sources for the 1.6 μm emission.

3. Possibility of a Low Loss Selenide Optical Fiber

The minimum transmission loss wavelength in chalcogenide glasses is usually determined by the intersection between the weak absorption tail and the multiphonon absorption tail in case the extrinsic vibrational impurity absorption does not exist [15]. Due to the reduced multiphonon absorption in such heavy glass fibers, the minimum loss wavelength is shifted to longer wavelength-side than that of the conventional oxide glass fibers. As a result, the magnitude of the weak absorption tail is almost responsible for the clarity of a selenide optical fiber at the 1.6 μm band. The weak absorption tail is caused by the additional band gap states, which are formed from electronic impurities such as transition metal elements or defects such as valence alternation pairs and dangling bonds [27]. In a highly pure and homogeneous glass, it is assumed that the band gap states caused by the defects is formed at the glass transition temperature during the melt quenching process [15]. Chalcogenide glasses are vulnerable to the formation of the defects in their electronic band gap [28]. Mainly because of the weak absorption, one can hardly anticipate a selenide optical fiber with a transmission loss comparable to that of the oxide glass fibers. However, the propagation loss of ~2 dB/m at the 1.6 μm band can be ascertained in the selenide glass fibers [29]. Fortunately, the additional extrinsic absorptions associated with the molecular vibra-tional species such as OH^- and SeH^- are not located at the 1.6 μm band if their concentration in the glasses is kept below a readily achievable limit [30].

The current host glass exhibits a superior thermal stability. Its glass transition and onset of crystallization temperatures are ~355 ℃ and ~510 ℃, respectively. Fiber drawing from the glass rods was successful [31]. About 5 m-long fiber with a diameter of ~120 μm was coated with a UV-curable polymer. Optical loss of ~9 dB/m was measured from the drawn fiber at 1313 nm with an Nd^{3+}: YLF laser by the conventional cut back method. Thus, elaboration on the materials purification is further needed. Drawing of a core/clad structured fiber is being tried. We anticipate that a mono-mode selenide optical fiber

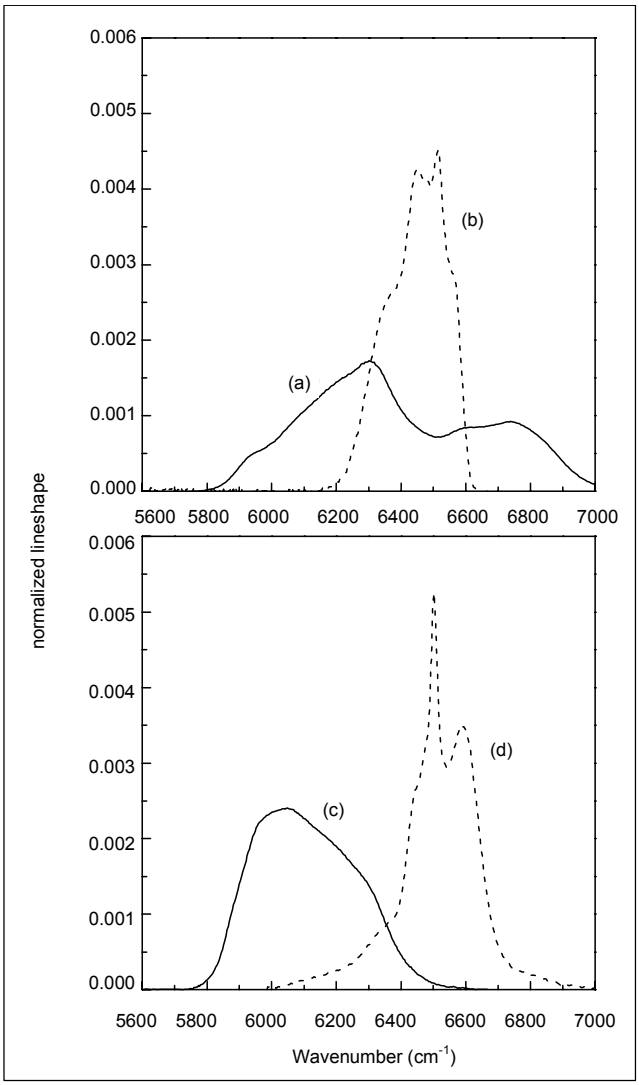

Fig. 8. Lineshape spectra of (a) absorption of Pr^{3+}, (b) emission of Er^{3+}, (c) emission of Pr^{3+} and (d) absorption of Er^{3+} in selenide glass. Note that the area under each spectrum is identical to each other.

with optical loss less than ~5 dB/m at the 1.6 μm band is quite promising mainly because of the good thermal stability of the host glasses used in this study. A numerical simulation regarding the Pr^{3+}-doped selenide fiber amplifiers indicates that a favorable optical gain may be achievable even in a 50 cm-long fiber, though the background transmission loss of the fiber is assumed to be 5 dB/m [31].

V. CONCLUSION

The measured peak wavelength and full-width at half-maximum of the 1.6 μm emission from Pr^{3+}: ($^3F_3$, $^3F_4$) → $^3H_4$ transition in Pr^{3+}- and Pr^{3+}/Er^{3+}-doped selenide glasses are ~1650 nm and ~120 nm, respectively. A moderate lifetime of

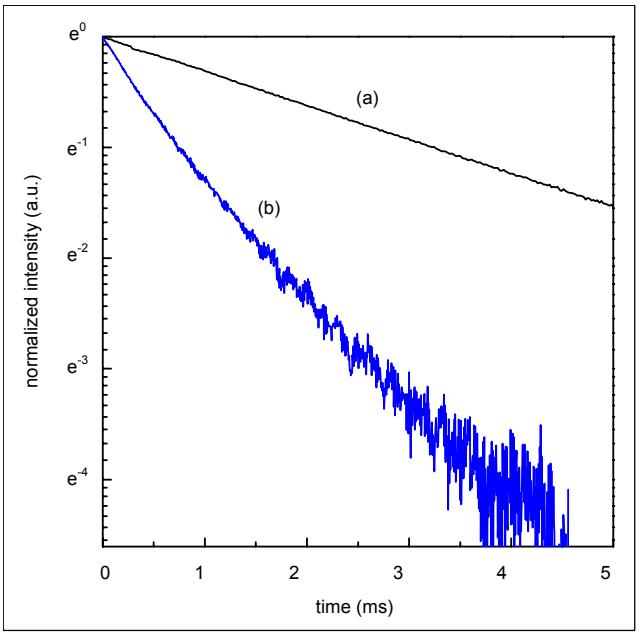

Fig. 9. Decay traces of 0.1 mol% Er^{3+}-doped selenide glasses of which Pr^{3+} concentration is (a) 0 and (b) 0.05 mol%.

the thermally coupled upper manifolds (~212 ± 10 μs) together with a high stimulated emission cross-section of ~$(3 \pm 1)\times 10^{-20}$ cm^2 promises to be useful for 1.6 μm band fiber-optic amplifiers that can be pumped with existing 1480 nm high-power laser diodes. Codoping of Er^{3+} into a Pr^{3+}-doped low phonon energy glass significantly enhanced the emission intensity by way of a nonradiative Er^{3+}: $^4I_{13/2}$ → Pr^{3+}: ($^3F_3$, $^3F_4$) energy transfer.

REFERENCES

[1] G.A. Thomas, B.I. Shraiman, P.F. Glodis, and M.J. Stephen, "Towards the Clarity Limit in Optical Fibre," *Nature (London)*, vol. 404, 2000, pp. 262-264.

[2] See, for example, papers in Optical Amplifiers and Their Applications, *OSA Trends in Optics and Photonics Series* (TOPS), vol. 16, edited by M.N. Zerras, A.E. Miller, and S. Sasaki (OSA, Washington DC, 1997), pp. 2–12.

[3] R.J. Mears, L. Reekie, I.M. Jauncey, and D.N. Payne, "Low-Noise Erbium-Doped Fiber Amplifier Operating at 1.54 μm," *Electron. Lett.*, vol. 23, 1987, pp. 1026-1028.

[4] Y. Ohishi, A. Mori, M. Yamada, H. Ono, Y. Nishida, and K. Oikawa, "Gain Characteristics of Tellurite-Based Erbium-Doped Fiber Amplifiers for 1.5-μm Broadband Amplification," *Opt. Lett.*, vol. 23, no. 4, 1998, pp. 274-276.

[5] B.H. Choi, M.J. Chu, H.H. Park, and J.H. Lee, "Performances of Erbium-Doped Fiber Amplifier Using 1530 nm-Band Pump for Long Wavelength Multichannel Amplification," *ETRI J.*, vol. 23, no. 1, 2001, pp. 1-8.

[6] H. Tawarayama, E. Ishikawa, K. Yamanaka, K. Itoh, K. Okada, H. Aoki, H. Yanagita, Y. Matsuoka, and H. Toratani, "Optical Ampli-

fication at 1.3 μm in a Praseodymium-Doped Sulfide Glass Fiber," *J. Am. Ceram. Soc.*, vol. 83, no. 4, 2000, pp. 792-796.

[7] D.T. Schaafsma, L.B. Shaw, B. Cole, J.S. Sanghera, and I.D. Aggarwal, "Modeling of Dy^{3+}-Doped GeAsSe Glass 1.3-μm Optical Fiber Amplifiers," *IEEE Photon. Technol. Lett.*, vol. 10, no. 11, 1998, pp. 1548-1550.

[8] T. Kasamatsu, Y. Yano, and H. Sekita, "1.50-μm-Band Gain-Shifted Thulium-Doped Fiber Amplifier with 1.05- and 1.56-μm Dual-Wavelength Pumping," *Opt. Lett.*, vol. 24, no. 23, 1999, pp. 1684-1686.

[9] T. Sakamoto, M. Shimizu, M. Yamada, T. Kanamori, Y. Ohishi, Y. Terunuma, and S. Sudo, "35-dB Gain Tm-Doped ZBLYAN Fiber Amplifier Operating at 1.65 μm," *IEEE Photon. Technol. Lett.*, vol. 8, no. 3, 1996, pp. 349-351

[10] S.H. Park, D.C. Lee, J. Heo, and H.S. Kim, "Pr^{3+}/Er^{3+} Codoped Ge-As-Ga-S Glasses as Dual-Wavelength Fiber-Optic Amplifiers for 1.31 and 1.55 μm Windows," *J. Am. Ceram. Soc.*, vol. 83, no. 5, 2000, pp. 1284-1286.

[11] S.R. Bowman, J. Ganem, B.J. Feldman, and A.W. Kueny, "Infrared Laser Characteristics of Praseodymium-Doped Lanthanum Trichloride," *IEEE J. Quantum Electron*, vol. 30, no. 12, 1994, pp. 2925-2928.

[12] L.B. Shaw, B.B. Harbison, B. Cole, J.S. Sanghera, and I.D. Aggarwal, "Spectroscopy of the IR Transitions in Pr^{3+} Doped Heavy Metal Selenide Glasses," *Opt. Express*, vol. 1, no. 4, 1997, pp. 87-96.

[13] Y.G. Choi and J. Heo, "1.3 μm Emission and Multiphonon Relaxation Phenomena in PbO-Bi_2O_3-Ga_2O_3 Glasses Doped with Rare-Earths," *J. Non-Cryst. Solids*, vol. 217, 1997, pp. 199-207.

[14] Y.G. Choi, K.H. Kim, S.H. Park, and J. Heo, "Comparative Study of Energy Transfers from Er^{3+} to Ce^{3+} in Tellurite and Sulfide Glasses under 980 nm Excitation," *J. Appl. Phys.*, vol. 88, no. 7, 2000, pp. 3832-3839.

[15] T. Kanamori, Y. Terunuma, and T. Miyashita, "Preparation of Chalcogenide Optical Fiber," *Rev. Electr. Commun. Lab.*, vol. 32, no. 3, 1984, pp. 469-477.

[16] P. Nêmec, B. Frumarová, and M. Frumar, "Structure and Properties of the Pure and Pr^{3+}-Doped $Ge_{25}Ga_5Se_{70}$ and $Ge_{30}Ga_5Se_{65}$ glasses," *J. Non-Cryst. Solids*, vol. 270, 2000, pp. 137-146.

[17] Y.G. Choi, K.H. Kim, B.J. Lee, Y.B. Shin, Y.S. Kim, and J. Heo, "Emission Properties of Er^{3+}: $^4I_{11/2} \rightarrow {}^4I_{13/2}$ Transition in Er^{3+}- and Er^{3+}/Tm^{3+}-Doped Ge-Ga-As-S Glasses," *J. Non-Cryst. Solids*, vol. 278, 2000, pp. 137-144.

[18] L.B. Shaw, S.R. Bowman, B.J. Feldman, and J. Ganem, "Radiative and Multiphonon Relaxation of the Mid-IR Transitions of Pr^{3+} in $LaCl_3$," *IEEE J. Quantum Electron*, vol. 32, no. 12, 1996, pp. 2166-2172.

[19] Y.G. Choi, K.H. Kim, and J. Heo, "Spectroscopic Properties of and Energy Transfer in PbO-Bi_2O_3-Ga_2O_3 Glass Doped with Er_2O_3," *J. Am. Ceram. Soc.*, vol. 82, no. 10, 1999, pp. 2762-2768.

[20] S.M. Kirkpatrick, S.R. Bowman, L.B. Shaw, and J. Ganem, "Cross Relaxation and Upconversion Coefficients of the Mid-Infrared Transitions of Pr^{3+}: $LaCl_3$," *J. Appl. Phys.*, vol. 82, no. 6, 1997, pp. 2759-2765.

[21] D.L. Dexter, "A Theory of Sensitized Luminescence in Solids," *J. Chem. Phys.*, vol. 21, no. 5, 1953, pp. 836-850.

[22] Y.G. Choi and J. Heo, "Influence of OH^- and Nd^{3+} Concentrations on the Lifetimes of the Nd^{3+}: $^4F_{3/2}$ Level in PbO-Bi_2O_3-Ga_2O_3 Glasses," *Phys. Chem. Glasses*, vol. 39, no. 6, 1998, pp. 311-317.

[23] R. Reisfeld and Y. Eckstein, "Energy Transfer between Tm^{3+} and Er^{3+} in Borate and Phosphate Glasses," *J. Non-Cryst. Solids*, vol. 11, 1973, pp. 261-284.

[24] D.R. Simons, A.J. Faber, and H. de Waal, "Pr^{3+}-Doped GeS_x-based Glasses for Fiber Amplifiers at 1.3 μm," *Opt. Lett.*, vol. 20, no. 5, 1995, pp. 468-470.

[25] D.W. Hewak, J.A. Medeiros Neto, B.Samson, R.S. Brown, K.P. Jedrzejewski, J. Wang, E. Taylor, R.I. Laming, G. Wylangowski, and D.N. Payne, "Quantum-Efficiency of Praseodymium Doped Ga:La:S Glass for 1.3 μm Optical Fibre Amplifiers," *IEEE Photon. Technol. Lett.*, vol. 6, no. 5, 1994, pp. 609-612.

[26] M.J.F. Digonnet and C.J. Gaeta, "Theoretical Analysis of Optical Fiber Laser Amplifiers and Oscillators," *Appl. Opt.*, vol. 24, no. 3, 1985, pp. 333-342.

[27] D.L. Wood and J. Tauc, "Weak Absorption Tails in Amorphous Semiconductors," *Phys. Rev. B*, vol. 5, no. 8, 1972, pp. 3144-3151.

[28] S. Ramachandran and S.G. Bishop, "Excitation of Er^{3+} Emission by Host Glass Absorption in Sputtered Films of Er-Doped $Ge_{10}As_{40}Se_{25}S_{25}$ glass," *Appl. Phys. Lett.*, vol. 73, no. 22, 1998, pp. 3196-3198.

[29] J.S. Sanghera and I.D. Aggarwal, "Active and Passive Chalcogenide Glass Optical Fibers for IR Applications: a review," *J. Non-Cryst. Solids*, vol. 256&257, 1999, pp. 6-16.

[30] G.G. Devyatykh, M.F. Churbanov, I.V. Scripachev, E.M. Dianov, and V.G. Plotnichenko, "The Role of Impurities in the Optical Losses of Chalcogenide Glass Fibers," *Proc. SPIE*, vol. 1048, 1989, pp. 80-84.

[31] Y.G. Choi, D.H. Cho, D.I. Chang, D.S. Lim, K.H. Kim, B.J. Park, and J. Heo, "Pr^{3+}-Doped Selenide Fiber for 1610~1650 nm Optical Amplifiers," *Proc. 26th ECOC*, Munich, Germany, Post Deadline Paper 2-1, 2000.

Yong Gyu Choi received the B.S. degree from KAIST in 1991.Then, he moved to POSTECH where he earned his M.S. and Ph.D. degrees in 1994 and in 1998, respectively. During the period of 1994 to 1998, his works were focused on processing and characterizing amorphous materials doped with rare-earth elements. Since he joined Telecommunication Basic Research Laboratory of ETRI in 1998, he has been involved in research in optical materials and devices for advanced optical communications. His current research interests include not only development of new optical fiber amplifiers and nonlinear fiber devices but also spectroscopic analysis of optical materials especially with X-ray absorption spectroscopy using synchrotron radiation.

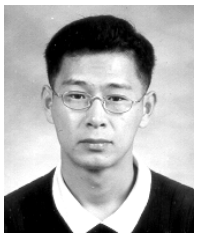

Bong Je Park received the B.S. degree from Hanyang University in 1999 and the M.S. degree from POSTECH in 2001. During the M.S. degree, his work was mainly about the process and characterization of non-silica materials doped with rare earth elements. After joining Telecommunication Basic Research Laboratory of ETRI in 2001 as a member of engineering staff, he has been involved in the development of new optical fiber amplifiers based on non-silica materials.

Kyong Hon Kim received the B.S. degree from Kyungpook National University in 1979 and the Ph.D. degree from State University of New York at Buffalo, USA in 1986, both in physics. During the period of 1986 to 1989, he worked in the area of dye and solid-state lasers and their application in space science at NASA Langley Research Center, and served as a research assistant professor in Hampton University, Virginia, USA. Since he joined Telecommunication Basic Research Laboratory of ETRI in 1989, he has been involved in fiber-optic device research for advanced optical communications. He is now in charge of technical management of optical communication device research activities based on fiber, semiconductor, and polymer materials.

Jong Heo received Ph.D. in materials science and engineering at University of California, Los Angeles in 1988. He was an assistant research professor at fiber optic materials research program at Rutgers University in USA before joining POSTECH in 1991. His research interests include non-oxide glasses for fiber-optic amplifiers, infrared-transmitting glasses and fibers, fiber-optic chemical sensors, and solid waste recycling.